Research On Lithium Battery Health State Prediction Model Based On Multimodal Signal Decomposition And Uncertainty Quantification Technology

Jiangjiang Li[1,2], Lijuan Feng[1,2*], Junyan Zhao[1,2], and Jingfen Li[1,2]

[1] School of Electronics and Electrical Engineering, Zhengzhou University of Science and Technology, 450064, Zhengzhou, China
[2] Zhengzhou Intelligent Safety Control Engineering Research Center for Unmanned Aerial Vehicles
[*] Corresponding author. E-mail: 857003841@qq.com

Received: Mar. 26, 2026; Accepted: May. 18, 2026

Precise estimation of lithium-ion battery State of Health (SOH) is essential for the safe and efficient operation of energy systems and electronic devices. However, nonlinear degradation, multimodal noise, and prediction uncertainty limit the accuracy and credibility of traditional models. To address this, we propose a novel SOH prediction model integrating multimodal signal decomposition and uncertainty quantification. First, Successive Variational Mode Decomposition (SVMD) separates degradation features from noise by decomposing multimodal monitoring signals (voltage, current, temperature, and EIS) into intrinsic modal functions (IMFs). Second, an AM-CNN-BiLSTM hybrid network extracts deep spatial-temporal features from the IMFs for preliminary SOH prediction. Third, an MCMC-based Bayesian inference framework quantifies prediction uncertainty (data noise, model parameters, and extraction errors), providing a probability distribution that improves overall model credibility. Validated on the NASA and Oxford datasets against traditional and advanced models (including Battery GPT), the proposed method outperformed comparisons, achieving an RMSE under 0.46%, a MAPE under 0.91%, and a determination coefficient above 0.991. Additionally, uncertainty quantification showed a prediction interval coverage probability (PICP) of 95.2% at a 95% confidence level. Ultimately, this model provides a high-precision, credible technical approach with strong engineering prospects for Battery Management Systems (BMS).

Keywords: Lithium battery; State of Health (SOH); Multimodal signal decomposition; Successive Variational Mode Decomposition (SVMD); Uncertainty quantification; Bayesian inference

http://dx.doi.org/10.6180/jase.202610_33.014

1. Introduction

With the rapid development of new energy technologies, lithium-ion batteries have become the core energy storage components in electric vehicles, grid-scale energy storage systems, and portable electronic devices, due to their high energy density, long cycle life, low self-discharge rate [1]. Nevertheless, lithium-ion batteries inevitably suffer performance degradation after prolonged charge–discharge cycling. Such aging behavior is mainly reflected in capacity fading, internal resistance growth, and reduced charge–discharge efficiency. This irreversible decay not only shortens battery service life but also introduces severe safety risks, including thermal runaway, fire and explosion hazards, thereby threatening the stable operation of the overall energy system [2]. State of Health (SOH) characterizes the current performance of a battery relative to its initial rated status, commonly defined as the ratio of present available capacity to the nominal capacity. It serves as a core indicator for quantitatively evaluating battery aging severity [3, 4]. Reliable and high-precision SOH estimation can support scientific maintenance scheduling, replacement decisions, and real-time safety early warning. Accordingly, it contributes greatly to enhancing the operational reliability of energy storage systems and lowering long-term operational costs [5].

Recently, State of Health (SOH) prediction for lithium-ion batteries has attracted extensive research attention, with existing approaches generally classified into three categories: model-driven, data-driven, and hybrid strategies. Model-based schemes, including equivalent circuit models and electrochemical models, correlate battery degradation behaviors with SOH by leveraging the internal electrochemical principles of lithium cells [6]. While such methods deliver clear interpretability, their practical application is constrained by intricate internal reaction mechanisms, difficult parameter calibration, and poor generalization under complex operating conditions—limiting their capability to support high-precision prediction in real-world scenarios [7]. By contrast, data-driven approaches, particularly deep learning-enabled techniques, have gained increasing popularity owing to their outstanding capacity in fitting nonlinear relationships and independence from sophisticated mathematical modeling [8]. Common deep learning models such as Long Short-Term Memory (LSTM), Convolutional Neural Network (CNN), and Transformer have been widely used in SOH prediction [9]. However, traditional data-driven methods still have obvious limitations: first, the monitoring signals of lithium batteries (voltage, current, temperature, etc.) are typical multimodal signals, which contain a lot of noise and redundant information, and directly inputting these signals into the model will lead to low feature extraction efficiency and poor prediction accuracy [10]; second, most existing models only output deterministic SOH prediction values, ignoring the uncertainty existing in the prediction process (such as data measurement noise, model parameter fluctuation, and feature extraction error), which makes it difficult to evaluate the credibility of the prediction results and limits the practical application of the model in safety-critical scenarios [11].

To solve the above problems, researchers have tried to introduce signal decomposition technology into SOH prediction to improve the quality of input data. Variational Mode Decomposition (VMD) is a commonly used adaptive signal decomposition method, which can decompose complex signals into multiple intrinsic modal functions (IMFs) with different frequency bands, effectively separating effective features from noise [12]. However, the VMD algorithm needs to manually set the number of modal components in advance, which is easy to cause modal aliasing or incomplete decomposition, affecting the effect of feature extraction. Successive Variational Mode Decomposition (SVMD), as an improved version of VMD, can adaptively determine the number of modal components and the optimal central frequency through iterative decomposition, avoiding the defects of VMD and improving the accuracy of signal decomposition. In terms of uncertainty quantification, Bayesian inference has been gradually applied to battery SOH prediction because it can effectively quantify the uncertainty of model parameters and prediction results by combining prior information and sample data [13]. However, the combination of multimodal signal decomposition, deep learning, and Bayesian uncertainty quantification is still in the exploratory stage, and there is a lack of a systematic framework to integrate these technologies to achieve high-precision and credible SOH prediction.

To address the aforementioned limitations, this paper develops a novel lithium-ion battery SOH prediction framework integrating multimodal signal decomposition and uncertainty quantification. The key contributions of this work are summarized as follows.

1. A SVMD-based multimodal signal decomposition method is proposed to decompose the complex monitoring signals of lithium batteries into multiple IMFs, which effectively removes noise interference and extracts key degradation features.

2. A hybrid deep learning network (AM-CNN-BiLSTM) is constructed to extract deep spatial-temporal features from the decomposed IMFs, which improves the ability of the model to capture the nonlinear degradation law of lithium batteries.

3. A Bayesian inference framework based on MCMC is introduced to quantify the uncertainty of the prediction results, providing a reliable basis for the evaluation of the prediction credibility.

2. Materials and methods

The overall architecture of our proposed SOH prediction model for lithium-ion batteries, which integrates multimodal signal decomposition and uncertainty quantification, is illustrated in Fig. 1. The entire framework consists of three core modules: multimodal signal decomposition based on SVMD, SOH preliminary prediction based on AM-CNN-BiLSTM, and uncertainty quantification based on Bayesian inference. The specific implementation process is as follows. First, we collect the multimodal monitoring signals of lithium batteries (voltage, current, temperature, EIS data), and preprocess the signals to eliminate outliers and normalize them. Second, we use SVMD to decompose the preprocessed multimodal signals into multiple IMFs, and select the effective IMFs containing key degradation features. Third, we input the effective IMFs into the AM-CNN-BiLSTM network to extract deep spatial-temporal features and output the preliminary deterministic SOH prediction value. Finally, we use the Bayesian inference framework based on MCMC to quantify the uncertainty of the prediction results, and output the probability distribution and prediction interval of the SOH value.

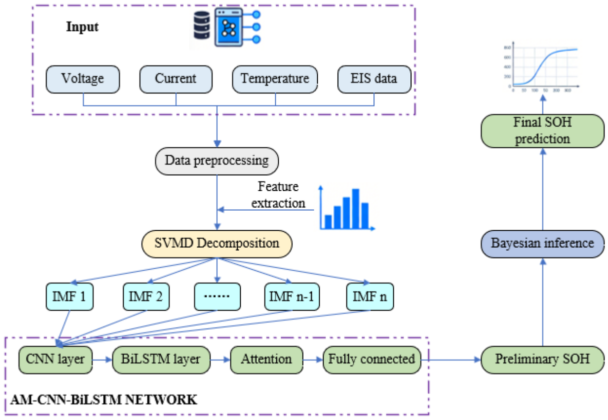

Fig. 1. Proposed lithium battery SOH prediction model.

2.1. Multimodal Signal Decomposition Based on SVMD

Successive Variational Mode Decomposition (SVMD) is an adaptive signal decomposition algorithm improved on the basis of VMD, which solves the problem that VMD needs to manually set the number of modal components [14]. SVMD works by iteratively decomposing the input signal, adaptively determining the mode number and optimal central frequencies, and ultimately separating the original signal into multiple IMF components with distinct time scales alongside one residual term. The mathematical formulation of SVMD is presented below.

$$\begin{cases} \min\limits_{u_n,\omega_n,f_r} \{\alpha J_1 + J_2 + J_3\} \\ \text{subject to: } u_n(t) + f_r(t) = f(t) \end{cases} \tag{1}$$

Where α is the balancing parameter. $f(t)$ is the input multimodal signal (such as battery voltage, current, or temperature signal). u_n and f_r are the n -th IMF and the residual component decomposed from $f(t)$, respectively. ω_n is the central frequency of the nth IMF. J_1, J_2, and J_3 are the constraint terms of the variational model, which are defined as follows.

$$J_1 = \left\| \partial_t \left(\left(\delta(t) + \frac{j}{\pi t} \right) * u_n(t) \right) e^{-j\omega_n t} \right\|_2^2 \tag{2}$$

$$J_2 = \|\beta_n(t) * f_r(t)\|_2^2 \tag{3}$$

$$J_3 = \sum_{i=1}^{L-1} \|\beta_i(t) * u_n(t)\|_2^2 \tag{4}$$

Where $\delta(t)$ is the Dirac function. $\beta_i(t)$ and $\beta_n(t)$ are the impulse responses of the filters. L is the number of iterative decompositions. The SVMD algorithm solves the above variational optimization problem through the Alternating Direction Method of Multipliers (ADMM), iteratively updates u_n, ω_n, and the dual variable λ, until the convergence condition is met, and finally obtains all IMFs and residual components.

In this study, the multimodal signals of lithium batteries (voltage, current, temperature, and EIS data) are decomposed by SVMD. Each type of signal is decomposed into multiple IMFs, and the Pearson correlation coefficient is used to select the IMFs with strong correlation with SOH (correlation coefficient absolute value > 0.8) as the input features of the subsequent prediction network, which effectively removes noise interference and reduces redundant information.

2.2. SOH Preliminary Prediction Based on AM-CNN-BiLSTM

To fully mine spatial and temporal feature information from decomposed IMF components, we construct a hybrid deep learning network integrating the attention mechanism (AM), CNN, and BiLSTM modules. The detailed structure of the proposed AM-CNN-BiLSTM network is illustrated in Fig. 2.

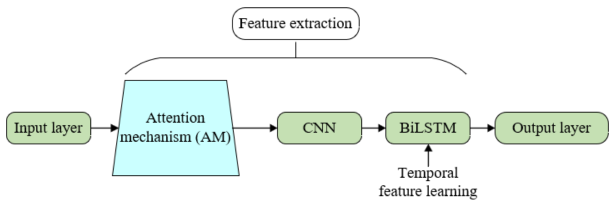

Fig. 2. Structure of the AM-CNN-BiLSTM network.

1. CNN Layer. The decomposed IMF components exhibit typical multidimensional time-series characteristics. The CNN module is adopted to extract spatial features from these signals, such as local fluctuation patterns, effectively capturing intrinsic local data correlations [15, 16]. This CNN architecture integrates convolutional layers, batch normalization modules, and max-pooling operations. One-dimensional convolution kernels perform feature convolution on the

input IMF sequences, while batch normalization accelerates model convergence and mitigates overfitting risks. Meanwhile, max-pooling downsamples the generated feature maps to reduce parameter volume while preserving critical spatial feature information.

2. BiLSTM Layer. The BiLSTM layer is composed of a forward LSTM and a backward LSTM, which can capture the temporal correlation of the data in both forward and backward directions, effectively solving the problem that traditional LSTM can only capture the forward temporal features [17].

3. Attention Mechanism (AM). The attention mechanism is introduced to dynamically assign adaptive weights to high-dimensional features extracted by the BiLSTM module. It strengthens critical information closely correlated with SOH estimation while suppressing irrelevant and redundant feature components. The detailed computational procedure of the attention module is presented below.

$$e_t = \tanh\left(W_a h_t + b_a\right) \tag{5}$$

$$\alpha_t = \frac{\exp\left(e_t^T u_a\right)}{\sum_{k=1}^{T} \exp\left(e_k^T u_a\right)} \tag{6}$$

$$h_{att} = \sum_{t=1}^{T} \alpha_t h_t \tag{7}$$

Where h_t is the output of the BiLSTM layer at time t. W_a and b_a are the weight matrix and bias term of the attention layer. u_a is the attention vector. α_t is the attention weight at time $t.h_{att}$ is the feature vector after attention weighting.

4. Fully Connected Layer. After weighted optimization via the attention module, the refined feature vector is fed into the fully connected layer. The model then outputs deterministic SOH estimation results with the activation functions of ReLU and Sigmoid adopted in succession. In this network, Mean Squared Error (MSE) is selected as the loss function, whose specific definition is presented below.

$$L_{MSE} = \frac{1}{N} \sum_{i=1}^{N} \left(SOH_{\text{true },i} - SOH_{\text{pred },i}\right)^2 \tag{8}$$

Where N is the number of samples. $SOH_{\text{true },i}$ is the true SOH value of the i-th sample, and $\text{SOH}_{\text{pred },i}$ is the predicted SOH value of the i-th sample.

2.3. Uncertainty Quantification Based on Bayesian Inference

To quantify the uncertainty inherent in SOH estimation outcomes, we adopt a Bayesian inference framework integrated with the Markov Chain Monte Carlo (MCMC) algorithm. Its core principle lies in updating the prior parameter distribution using sampled data to derive the posterior distribution; the probability distribution of final predictions can then be further inferred from such posterior results [18].

In this study, the parameters of the AM-CNN-BiLSTM network are regarded as random variables, and the prior distribution of the parameters is set as a Gaussian distribution $p(\theta) \sim \mathcal{N}(\mu_0, \Sigma_0)$, where θ is the parameter set of the network, μ_0 is the prior mean, and Σ_0 is the prior covariance matrix. The likelihood function of the model is constructed based on the MSE loss function, which is defined as follows.

$$p(y \mid \theta, X) \sim \mathcal{N}\left(f_\theta(X), \sigma^2 I\right) \tag{9}$$

Where X is the input feature matrix (effective IMFs). y is the true SOH value. $f_\theta(X)$ is the output of the AM-CNN-BiLSTM network. σ^2 is the noise variance, and I is the identity matrix.

According to Bayes' theorem, the posterior distribution of the parameters θ is:

$$p(\theta \mid y, X) \propto p(y \mid \theta, X) p(\theta) \tag{10}$$

Since the posterior distribution of the parameters is complex and cannot be solved analytically, the MCMC algorithm (specifically the NUTS algorithm) is used to sample the posterior distribution of the parameters, and a large number of parameter samples are obtained. For a new input sample X_{new} , the prediction distribution of the SOH value is obtained by inputting the parameter samples into the AM-CNN-BiLSTM network.

$$\begin{aligned} & p\left(SOH_{\text{new}} \mid X_{\text{new}}, y, X\right) \\ & = \int p\left(SOH_{\text{new}} \mid X_{\text{new}}, \theta\right) p(\theta \mid y, X) d\theta \end{aligned} \tag{11}$$

The mean value derived from the predicted probability distribution is adopted as the final SOH estimation result. Meanwhile, the 95% prediction interval is calculated according to the corresponding quantiles, so as to quantitatively characterize the prediction uncertainty. Two evaluation indicators, namely Prediction Interval Coverage Probability (PICP) and Prediction Interval Average Width (PIAW), are introduced to assess the performance of uncertainty quantification, with their definitions presented below:

$$\text{PICP} = \frac{1}{N_{\text{test}}} \sum_{i=1}^{N_{\text{test}}} I\left(\text{SOH}_{\text{true},i} \in [L_i, U_i]\right) \quad (12)$$

$$\text{PIAW} = \frac{1}{N_{\text{test}}} \sum_{i=1}^{N_{\text{test}}} (U_i - L_i) \quad (13)$$

Where N_{test} is the number of test samples. $[L_i, U_i]$ is the 95% prediction interval of the i-th test sample. $I(\cdot)$ is the indicator function. A higher PICP and a lower PIAW indicate better uncertainty quantification effect.

2.4. Overall Model Flow

The specific steps are as follows.

1. Data Collection and Preprocessing. Collect the multimodal monitoring signals (voltage, current, temperature, EIS data) of lithium batteries during charge-discharge cycles, eliminate outliers through the 3α principle, and normalize the signals to the range [0,1] using the min-max normalization method to avoid the influence of different units on the model training.

2. Multimodal Signal Decomposition. Use SVMD to decompose each preprocessed signal into multiple IMFs and a residual component, calculate the Pearson correlation coefficient between each IMF and SOH, and select the IMFs with absolute correlation coefficient > 0.8 as effective features.

3. Preliminary SOH Prediction. Input the effective IMFs into the AM-CNN-BiLSTM network, train the network using the training set, and output the preliminary deterministic SOH prediction value on the test set.

4. Uncertainty Quantification. Use the MCMC algorithm to sample the posterior distribution of the AM-CNN-BiLSTM network parameters, obtain the prediction distribution of the SOH value, calculate the 95% prediction interval, and evaluate the uncertainty quantification effect using PICP and PIAW.

5. Model Evaluation. Evaluate the prediction accuracy of the model using RMSE, MAPE, and R^2, and compare it with the comparison models to verify the superiority of the proposed model.

3. Results and discussion

To validate the effectiveness and superiority of the developed model, comprehensive experiments are conducted on two public lithium-ion battery datasets from NASA and Oxford University. The experimental setup, dataset introduction, parameter configurations, and result analyses are elaborated in the following sections.

3.1. Experimental Environment and Dataset Description

3.1.1. Experimental Environment

The experimental environment is configured as follows: CPU: Intel Core i7-12700H (2.7GHz), GPU: NVIDIA RTX 3060 (6GB), memory: 16GB, operating system: Windows 11, programming language: Python 3.8, deep learning framework: PyTorch 1.12.0. The used main libraries include NumPy, Pandas, Matplotlib, Scikit-learn, and PyMC3 (for MCMC sampling).

3.1.2. Dataset Description

1. NASA Battery Dataset. The dataset is provided by the NASA Ames Research Center, which includes 8 18650-type lithium-ion batteries (B5, B6, B7, B18, B29, B30, B31, B32) with a rated capacity of 2.0Ah [19]. Battery cycling tests are conducted under diverse charging-discharging protocols, including constant current–constant voltage charging and constant current discharging. The monitored multimodal signals cover voltage, current, temperature, and capacity, the latter adopted for SOH calculation. Here, the battery end-of-life (EOL) is defined as the capacity decaying to 70% of its rated value (1.4 Ah). For experimental validation, each battery's dataset is split into a 70% training subset and a 30% testing subset.

2. Oxford Battery Dataset. The dataset is provided by the University of Oxford, which includes 4 soft-pack lithium-ion batteries (Cell1, Cell2, Cell3, Cell4) with a rated capacity of 0.74Ah [20]. The batteries are cycled under different environmental temperatures and charge-discharge rates, and the monitoring signals include voltage, current, temperature, and EIS data.

3.2. Model Parameter Settings

The parameters of the proposed model are set through cross-validation (5-fold cross-validation), and the specific settings are as follows.

SVMD parameters include balancing parameter $\alpha = 2000$, convergence threshold $\epsilon = 10^{-7}$, maximum number of iterations $= 1000$.

AM-CNN-BiLSTM parameters include CNN layer (1D convolution kernel size = 3, number of convolution kernels $= 64$, batch normalization momentum $= 0.9$, max-pooling size $= 2$), BiLSTM layer (number of hidden units $= 128$, dropout rate $= 0.3$), Attention layer (attention vector dimension $= 64$), the fully connected layers are configured with 64 neurons in the hidden layer and one neuron for the output layer. The Adam optimizer is adopted, with a learning rate of 0.001 , a batch size of 32 , and the training process set to 100 epochs.

Bayesian Inference Parameters contain $\mathcal{N}(0, 0.01\mathrm{I})$, noise variance $\sigma^2 = 0.001$, MCMC sampling number $= 2000$, burn-in period $= 500$.

3.3. Comparison Models

To verify the superiority of the proposed model, the following 5 comparison models are selected for experimental comparison:

Model 1. LSTM: Traditional LSTM model, directly inputting the preprocessed multimodal signals for SOH prediction.

Model 2. CNN-LSTM: Hybrid model combining CNN and LSTM, inputting the preprocessed multimodal signals.

Model 3. VMD-BiLSTM: Using VMD to decompose the signals, then inputting the IMFs into BiLSTM for prediction.

Model 4. AT-CNN-BiLSTM: Attention-based CNN-BiLSTM model proposed in literature [21].

Model 5: Battery GPT. Transformer-based early degradation prediction model proposed in literature [22].

3.4. Experimental Results and Analysis

3.4.1. Prediction Accuracy Analysis

The prediction accuracy metrics (RMSE, MAPE, R^2) of the proposed model and the comparison models on the NASA battery dataset and Oxford battery dataset are shown in Tables 1 and 2, respectively. The smaller the RMSE and MAPE, the larger the R^2, indicating better prediction accuracy.

It can be seen from Tables 1 and 2 that the proposed model achieves the best prediction accuracy on both datasets. Compared with the traditional LSTM model, the RMSE and MAPE of the proposed model are reduced by 69.1% and 61.1% on the NASA dataset, and 66.0% and 54.7% on the Oxford dataset, respectively. Compared with the advanced Battery GPT model, the RMSE and MAPE of the proposed model are reduced by 22.4% and 21.7% on the NASA dataset, and 16.4% and 7.1% on the Oxford dataset, respectively. The main reasons for the superior performance of the proposed model are as follows: (1) SVMD can adaptively decompose the multimodal signals, effectively remove noise interference, and extract key degradation features; (2) The AM-CNN-BiLSTM network can fully capture the spatial and temporal features of the decomposed IMFs, improving the ability to model the nonlinear degradation law of lithium batteries; (3) The Bayesian inference framework can effectively correct the model prediction deviation, further improving the prediction accuracy.

To intuitively visualize the estimation performance, Fig. 3 and Fig. 4 illustrate the SOH fitting curves of our method and comparative models for the B7 cell from the NASA dataset and Cell2 from the Oxford dataset, respectively. As observed from the graphical results, the curve generated by the proposed model maintains a higher consistency with the real SOH degradation trend, especially in the late stage of battery degradation (when the capacity drops rapidly), the proposed model still maintains high prediction accuracy, while the comparison models have obvious prediction deviations.

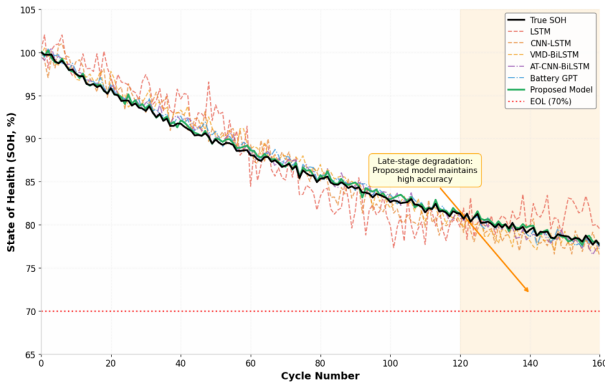

Fig. 3. SOH prediction curve of B7 battery (NASA dataset).

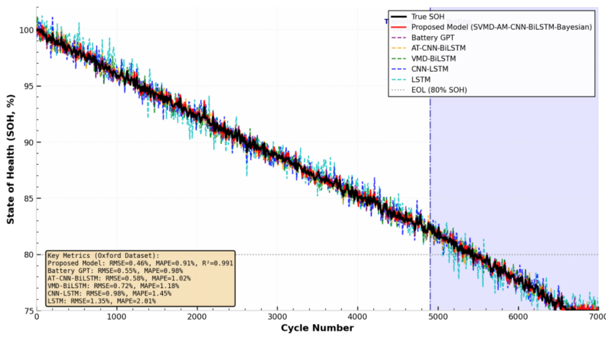

Fig. 4. SOH prediction curve of Cell2 battery (Oxford dataset).

3.4.2. Uncertainty Quantification Analysis

The uncertainty quantification results of the proposed model on the two datasets are shown in Table 3. The PICP and PIAW are used to evaluate the effect of uncertainty quantification. It can be seen from Table 3 that the PICP of the proposed model on both datasets is close to 95% (the target confidence level), and the PIAW is small, indicating that the proposed model can effectively quantify the uncertainty of the prediction results, and the prediction interval is reliable and compact.

The 95% prediction interval of the proposed model on the B7 battery (NASA dataset) is shown in Fig. 5. It can be

Table 1. Prediction accuracy metrics on NASA battery dataset (%).

Model	RMSE	MAPE	R^2
LSTM	1.23 ± 0.15	1.85 ± 0.21	0.962 ± 0.013
CNN-LSTM	0.87 ± 0.11	1.32 ± 0.18	0.978 ± 0.009
VMD-BiLSTM	0.65 ± 0.09	1.05 ± 0.15	0.985 ± 0.007
AT-CNN-BiLSTM	0.52 ± 0.08	0.95 ± 0.12	0.989 ± 0.005
Battery GPT	0.49 ± 0.07	0.92 ± 0.11	0.990 ± 0.004
Proposed Model	0.38 ± 0.06	0.72 ± 0.10	0.993 ± 0.003

Table 2. Prediction accuracy metrics on Oxford battery dataset (%).

Model	RMSE	MAPE	R^2
LSTM	1.35 ± 0.17	2.01 ± 0.23	0.958 ± 0.015
CNN-LSTM	0.98 ± 0.12	1.45 ± 0.19	0.975 ± 0.010
VMD-BiLSTM	0.72 ± 0.10	1.18 ± 0.16	0.983 ± 0.008
AT-CNN-BiLSTM	0.58 ± 0.09	1.02 ± 0.13	0.988 ± 0.006
Battery GPT	0.55 ± 0.08	0.98 ± 0.12	0.989 ± 0.005
Proposed Model	0.46 ± 0.07	0.91 ± 0.11	0.991 ± 0.004

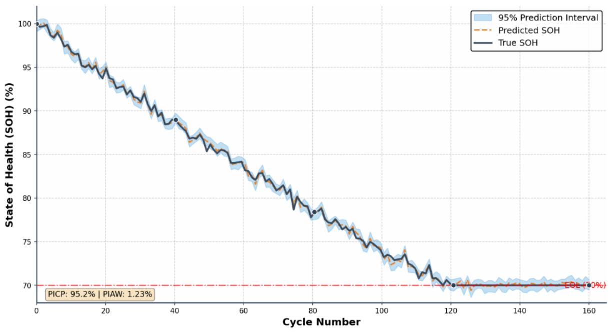

Fig. 5. 95% prediction interval of B7 battery (NASA dataset).

Table 3. Prediction accuracy metrics on NASA battery dataset (%).

Dataset	PICP (%)	PIAW (%)
NASA Battery Dataset	95.2 ± 0.8	1.23 ± 0.15
Oxford Battery Dataset	94.8 ± 0.9	1.35 ± 0.17

seen from the figure that most of the true SOH values are within the 95% prediction interval, and the prediction interval is compact, which indicates that the proposed model can not only provide accurate SOH prediction values but also quantify the reliability of the prediction results, providing a basis for practical engineering applications (such as battery maintenance and safety early warning).

3.4.3. Robustness Analysis

To verify the robustness of the proposed model, Gaussian noise with different signal-to-noise ratios (SNR = 20dB, 15dB, 10dB) is added to the multimodal monitoring signals of the test set, and the prediction accuracy of the proposed model and the comparison models is tested. The results are shown in Fig. 6. It can be seen from the figure that with the decrease of SNR (i.e., the increase of noise interference), the prediction accuracy of all models decreases, but the proposed model still maintains the highest prediction accuracy. When SNR = 10dB (severe noise interference), the RMSE of the proposed model is 0.87% and 0.95% on the NASA and Oxford datasets, respectively, which is significantly lower than that of the comparison models. This indicates that the proposed model has strong robustness to noise interference, which is mainly due to the SVMD algorithm's ability to effectively separate noise from effective features, reducing the impact of noise on the model prediction.

4. Conclusions

This study proposes a novel lithium battery SOH prediction model integrating multimodal signal decomposition and uncertainty quantification technology to address the challenges of nonlinear degradation mechanisms, multimodal noise interference, and prediction uncertainty in traditional SOH prediction methods. The proposed model combines SVMD-based signal decomposition, AM-CNN-BiLSTM deep learning network, and Bayesian inference framework based on MCMC sampling to achieve high-precision and credible SOH prediction. Experimental results on NASA and Oxford battery datasets demonstrate that the proposed model achieves superior prediction performance with RMSE less than 0.46%, MAPE less than 0.91%, and R^2 greater than 0.991 , significantly outperforming traditional models (LSTM, CNN-LSTM, VMD-BiLSTM) and advanced models (AT-CNN-BiLSTM, Battery GPT). The proposed model provides a new technical approach

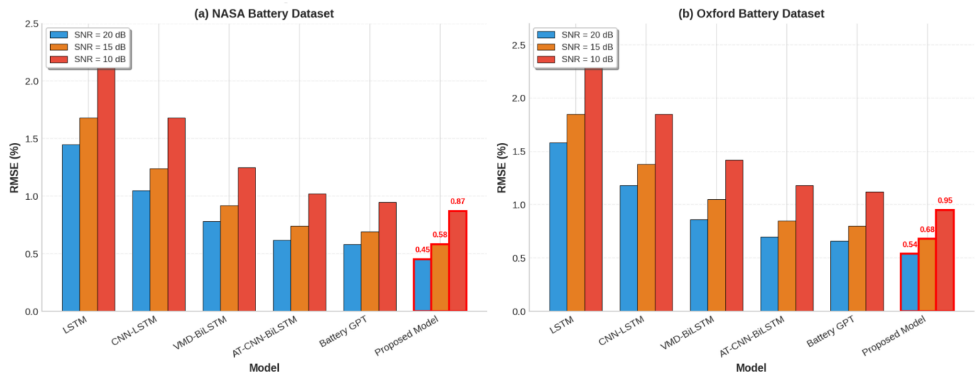

Fig. 6. Robustness test results of different models under different SNR.

for high-precision SOH prediction with uncertainty quantification, offering important theoretical value and practical engineering prospects for battery management systems in electric vehicles, energy storage systems, and portable electronic devices. Future research will focus on extending the model to multi-cell battery pack SOH prediction, exploring online adaptive learning strategies, and integrating physics-informed neural networks to further enhance model interpretability and generalization capabilities across diverse operating conditions.

Acknowledgement

This work supported by the Key Scientific Research Project Plan of Henan Province Higher Education Institutions (Project No. 26A413009).

References

[1] A. Pazhouheshgar, P. N. Nowruzmahaleh, A. Shokrieh, A. Barati, I. Soluki, M. Shokrieh, Z. Wei, and T. Yao, (2026) *"Mechanical characterization of flexible lithium-ion battery components: A multi-testing strategy"* **Journal of Energy Storage** ***156***: 121599. DOI: 10.1016/j.est.2026.121599.

[2] Y. Wu, X. Long, L. Li, L. Liu, Y. Wu, and Z. Zeng, (2026) *"Construction of high-mass loading dry-pressed lithium-ion battery electrodes with excellent flexibility via one-dimensional carbon nanomaterials"* **Journal of Energy Storage** ***156***: 121668. DOI: 10.1016/j.est.2026.121668.

[3] J. Lu, R. Xiong, J. Tian, C. Wang, and F. Sun, (2023) *"Deep learning to estimate lithium-ion battery state of health without additional degradation experiments"* **Nature Communications** ***14***(1): 2760. DOI: 10.1038/s41467-023-38458-w.

[4] G. Nuroldayeva, Y. Serik, D. Adair, B. Uzakbaiuly, and Z. Bakenov, (2023) *"State of health estimation methods for lithium-ion batteries"* **International Journal of Energy Research** ***2023***(1): 4297545. DOI: 10.1155/2023/4297545.

[5] Y. Li, S. Zhong, Q. Zhong, and K. Shi, (2019) *"Lithium-ion battery state of health monitoring based on ensemble learning"* **IEEE access** ***7***: 8754–8762. DOI: 10.1109/ACCESS.2019.2891063.

[6] S. Amir, M. Gulzar, M. O. Tarar, I. H. Naqvi, N. A. Zaffar, and M. G. Pecht, (2022) *"Dynamic equivalent circuit model to estimate state-of-health of lithium-ion batteries"* **Ieee Access** ***10***: 18279–18288. DOI: 10.1109/ACCESS.2022.3148528.

[7] C. Li, L. Yang, Q. Li, Q. Zhang, Z. Zhou, Y. Meng, X. Zhao, L. Wang, S. Zhang, Y. Li, et al., (2024) *"SOH estimation method for lithium-ion batteries based on an improved equivalent circuit model via electrochemical impedance spectroscopy"* **Journal of Energy Storage** ***86***: 111167. DOI: 10.1016/j.est.2024.111167.

[8] G. Sun, Y. Liu, and X. Liu, (2025) *"A method for estimating lithium-ion battery state of health based on physics-informed machine learning"* **Journal of Power Sources** ***627***: 235767. DOI: 10.1016/j.jpowsour.2024.235767.

[9] S. Peng, Y. Sun, D. Liu, Q. Yu, J. Kan, and M. Pecht, (2023) *"State of health estimation of lithium-ion batteries based on multi-health features extraction and improved long short-term memory neural network"* **Energy** ***282***: 128956. DOI: 10.1016/j.energy.2023.128956.

[10] Y. Tan and G. Zhao, (2019) *"Transfer learning with long short-term memory network for state-of-health prediction of lithium-ion batteries"* **IEEE Transactions on Industrial Electronics** ***67***(10): 8723–8731. DOI: 10.1109/TIE.2019.2946551.

[11] Z. Zhang, H. Min, H. Guo, Y. Yu, W. Sun, J. Jiang, and H. Zhao, (2023) *"State of health estimation method for lithium-ion batteries using incremental capacity and long short-term memory network"* **Journal of Energy Storage *64***: 107063. DOI: 10.1016/j.est.2023.107063.

[12] N. Xiang, T. Zhang, and Y. Liu, (2025) *"State of health prediction for lithium-ion batteries using extended long short-term memory network and frequency enhanced channel attention mechanism with variational mode decomposition"* **Measurement *249***: 117084. DOI: 10.1016/j.measurement.2025.117084.

[13] L. Hu, W. Wang, and G. Ding, (2023) *"RUL prediction for lithium-ion batteries based on variational mode decomposition and hybrid network model"* **Signal, Image and Video Processing *17***(6): 3109–3117. DOI: 10.1007/s11760-023-02532-z.

[14] Y. Liu, X. Hou, and Y. Xu, (2026) *"Battery state-of-health prediction based on feature extraction and a variational mode decomposition–temporal convolutional network–bidirectional long short-term memory network–self-attention model"* **Journal of Energy Storage *156***: 121629. DOI: 10.1016/j.est.2026.121629.

[15] S. Yin, H. Li, M. Ivanović, T. Chen, and L. Teng, (2026) *"FNNMFF: Crop pests and diseases detection based on fuzzy neural network and multilevel feature fusion in remote sensing images"* **Computer Science and Information Systems** (00): 12–12. DOI: 10.2298/CSIS251109012Y.

[16] S. Yin, L. Wang, T. Chen, H. Huang, J. Gao, J. Zhang, M. Liu, P. Li, and C. Xu, (2026) *"LKAFormer: A lightweight kolmogorov-arnold transformer model for image semantic segmentation"* **ACM Transactions on Intelligent Systems and Technology *17***(3): 1–24. DOI: 10.1145/3759254.

[17] Y. Jiang and S. Yin, (2023) *"Heterogenous-view occluded expression data recognition based on cycle-consistent adversarial network and K-SVD dictionary learning under intelligent cooperative robot environment"* **Computer Science and Information Systems *20***(4): 1869–1883. DOI: 10.2298/CSIS221228034J.

[18] J.-H. Kim, E. Kwak, J. Jeong, and K.-Y. Oh, (2023) *"Physics-informed Markov chain model to identify degradation pathways of lithium-ion cells"* **IEEE Transactions on Transportation Electrification *10***(2): 3468–3481. DOI: 10.1109/TTE.2023.3302433.

[19] H. Xu, Y. Peng, and L. Su. "Health state estimation method of lithium ion battery based on NASA experimental data set". In: *IOP Conference Series: Materials Science and Engineering*. ***452***. 3. IOP Publishing. 2018, 032067. DOI: 10.1088/1757-899X/452/3/032067.

[20] M. A. Khan, S. Thatipamula, L. Tresca, L. Xu, A. Trewartha, and S. Onori, (2025) *"High-power lithium-ion battery characterization dataset for stochastic battery modeling"* **Scientific Data *12***(1): 1506. DOI: 10.1038/s41597-025-05725-y.

[21] Q. Xing, X. Sun, Y. Fu, and K. Wang, (2025) *"Lithium-ion battery health estimate based on electrochemical impedance spectroscopy and CNN-BiLSTM-Attention"* **Ionics *31***(2): 1389–1403. DOI: 10.1007/s11581-024-05982-8.

[22] D. Zhou, Y. Sun, Q. Hu, Y. Shi, J. Yu, and J. Zhang, (2025) *"Generative pre-trained transformers (GPT) for lithium-ion battery charging state prediction in battery swapping station"* **Sustainable Energy Technologies and Assessments *82***: 104526. DOI: 10.1016/j.seta.2025.104526.